Immobilization of Carbon Nanotubes on Au(111) via Self-assembled Monolayers

Tomoaki Nishino,*[1] Satoshi Kanata,[2] and Chiyo Hirata[2]
[1]Nanoscience and Nanotechnology Research Center, Osaka Prefecture University,
1-2 Gakuencho, Naka-ku, Sakai, Osaka 599-8570
[2]Department of Physics and Electronics, Osaka Prefecture University,
1-1 Gakuencho, Naka-ku, Sakai, Osaka 599-8531

(Received July 25, 2011; CL-110625; E-mail: t-nishino@21c.osakafu-u.ac.jp)

We investigated the immobilization of single-walled carbon nanotubes on self-assembled monolayers (SAMs) on Au(111) by atomic force microscopy. The nanotubes were homogeneously attached to the SAMs of aminothiophenol and benzenethiol. We found that the nanotubes formed mesh-like structures on a 1-propanethiol SAM, which most likely reflected a weak interaction between the nanotubes and the SAM surface. These results demonstrate that the chemical functionality of a SAM surface strongly affected the immobilization of carbon nanotubes.

Single-walled carbon nanotubes (SWNTs) possess a rich variety of intriguing electronic properties,[1] which make SWNTs an ideal candidate for a wide range of applications, including electronic devices,[2–4] sensors,[5,6] and photovoltaics.[7,8] For fabricating such functional nanodevices, it is critical to assemble SWNTs on a solid surface in a controlled manner. Several methods have been explored for SWNT assembly on surfaces.[9,10] The reported techniques include electric- or magnetic-field-assisted processes,[11–13] DNA templates,[14,15] gas-flow alignment,[16,17] and Langmuir–Blodgett techniques.[18,19] In addition, self-assembled monolayers (SAMs) have been demonstrated to provide a useful means to attach SWNTs on their surfaces.[20,21] A controlled assembly of SWNTs having a sub-100-nm resolution was realized by using patterned SAMs.[22] Moreover, the chirality separation of nanotubes could be achieved on SAMs.[23] Despite these advantages of SAMs with respect to the assembly of SWNTs, knowledge about the SWNT immobilization on the SAMs is still limited. In this study, we investigated the effects of the surface chemistry of SAMs on the SWNT assembly. Three types of SAMs—4-aminothiophenol (4AT), benzenethiol (BT), and 1-propanethiol (1PT)—were employed for the SWNT immobilization. We demonstrated that the alignment and density of the nanotubes could be controlled by a rational design of the SAM functionality.

SWNTs produced by the HiPco process (Carbon Nanotechnologies Inc.) were oxidized in H_2SO_4/HNO_3 for 6 h, followed by a thorough wash with pure water and drying in vacuo. The oxidized SWNTs were dispersed in N-methylpyrrolidone at a concentration of 1, 0.1, or 0.01 mg mL^{-1} by ultrasonication. The nanotubes can be stably dispersed in this solvent without any surfactants.[24] The absence of surfactants allowed for investigations into the adsorption properties arising directly from SWNT–SAM interactions. An atomically flat Au(111) thin layer (thickness: 200 nm) was prepared by the thermal evaporation of Au onto mica under vacuum. The microscope glasses were glued onto the Au layer with Epotek 377 (Epoxy Technology), and these assemblies were heated at
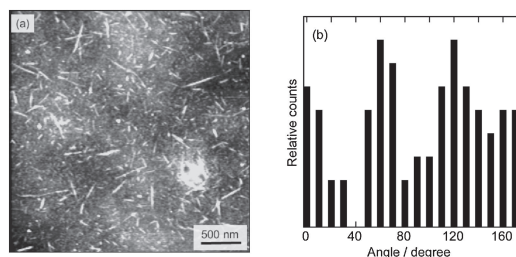

Figure 1. (a) AFM image of SWNTs spin-coated on the 4AT SAM at 4000 rpm using 1 mg mL^{-1} SWNT solution. (b) Histogram of the nanotube alignment. Each angle was measured relative to an arbitrary direction.

150 °C in an electric oven for 1.5 h. The mica sheet was stripped off to expose an ultraflat clean Au(111) surface.[25] The Au(111) substrate was modified with SAMs of 4AT, BT, or 1PT by immersing the substrate into the ethanol solution of the thiol at a concentration of 7.5 mM overnight. The SWNTs were spin-coated on the SAM surfaces, and the immobilized SWNTs were observed by atomic force microscopy (AFM, Seiko Instruments Inc., SPI3800-SPA400).

First, the 4AT-modified Au(111) surface was used as the substrate for the spin coating. The 1-mg mL^{-1} SWNT-dispersed solution was placed on the modified surface that was rotating at 4000 rpm, and AFM observations were performed to observe the immobilized nanotubes (Figure 1a). The AFM image showed that tubular structures densely covered the substrate surface, instead of the terrace–step structures found on the unmodified Au surface. These tubes were ascribed to single SWNTs or SWNT bundles containing a few SWNTs. Previously, we reported the observation of similarly immobilized SWNTs on the 4AT-modified Au(111) surface by means of scanning tunneling microscopy (STM).[26] The STM observation revealed that a large number of individual nanotubes were dispersed on the surface and that atomic resolution could be achieved for these nanotubes even under ambient conditions.

It is known that molecules bearing amino functional groups form favorable chemical interactions with the SWNT surface. For example, it was reported that nanotubes can be stably dispersed in amine solvents,[24,27] and this SWNT dispersibility was ascribed to the significant interaction between the SWNT and amine nitrogen.[28] It is proposed that amines form charge-transfer interactions with SWNTs. The charge transfer is evidenced by the modulated electrical conductance of the nanotubes upon the amine adsorption.[28] Furthermore, such interaction was found to be useful for immobilizing the SWNTs on solid surfaces, e.g., SiO$_2$ modified with aminopropyltrieth-
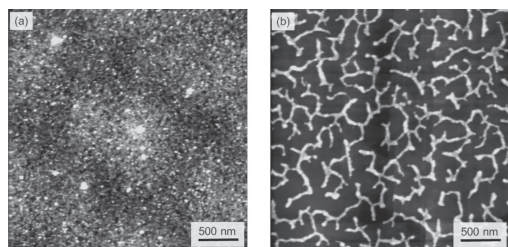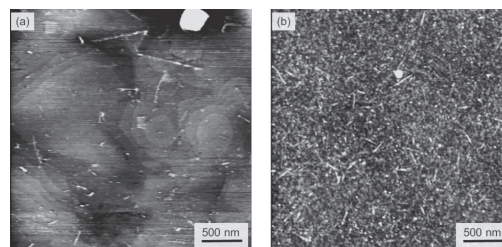
Figure 2. AFM images of SWNTs immobilized on (a) BT and (b) 1PT SAMs. Spin coatings were performed at 4000 rpm with 1 mg mL^{-1} SWNT solutions.

Figure 3. AFM images of SWNTs immobilized on (a) 4AT and (b) BT SAMs. Spin coatings were performed at 4000 rpm with 0.1 mg mL^{-1} SWNT solutions.

oxysilane.[20,21,23] On the basis of these studies, we concluded that the successful immobilization of the SWNTs on the 4AT-modified Au surfaces was due to the favorable interaction between the amino groups of the 4AT SAMs and the nanotube surfaces.

The alignment of the SWNTs on the Au(111) surface was examined using the AFM image shown in Figure 1a. The angle of each nanotube axis with respect to an arbitrary direction was measured to construct the histogram shown in Figure 1b. Interestingly, the histogram exhibited three distinct peaks that were equally separated from each other, demonstrating that the nanotube adsorption exhibited a threefold symmetry. It is known that the 4AT forms a closely packed SAM having the same threefold symmetry as the underlying Au(111) substrate.[29] Therefore, the observation of the threefold symmetry of the nanotube alignment supported our conclusion that the SWNT immobilization was due to the interaction between the SWNT and the 4AT.

The effect of the surface chemistry on the SWNT adsorption was investigated by using the Au surface modified with BT (Figure 2a) and 1PT SAMs (Figure 2b). In each case, 1-mg mL^{-1} SWNT solution was spin-coated onto the surface at 4000 rpm. When the BT-modified surface was used as the substrate, the AFM image exhibited a significantly dense adsorbed layer of the SWNTs (Figure 2a). In contrast to Figure 1a, the tubular structures of the SWNTs were hardly observed in the AFM images. This result was interpreted as the highly crowded adsorption of the SWNTs on the BT-modified surface. Under such circumstances, the SWNTs were interwoven with each other on the substrate surface, and individual nanotubes or their thin bundles could not adsorb with their tube axes completely parallel to the surface. The numerous bright spots seen in Figure 2a were ascribed to the SWNTs terminals protruding to the outermost surface of the adsorbed layer. In fact, the tubular structures could be observed on the BT-modified surface when the surface concentration of the SWNTs was decreased (see below). A noticeable difference in the adsorption behavior was found on the 1PT-modified surface (Figure 2b). While the nanotubes were uniformly dispersed in the adsorbed layer on the 4AT- and BT-modified surfaces (Figures 1a and 2a, respectively), mesh-like structures were found on the 1PT-modified surface. We attributed the formation of these structures to the partial aggregation of the SWNTs during the spin-coating procedure. The white lines that form the mesh-like structures were assigned as the bundled nanotubes, and the dark background between these nanotubes was the uncovered 1PT SAM surface.

As described above, amino groups were exposed at the outermost surface of the 4AT SAM, and a strong interaction between the amino group and the SWNT resulted in the immobilization of the SWNTs on the substrate surface. On the other hand, phenyl groups existed on the surface of the BT SAM. It was reported that aromatic molecules interact and bind to the SWNTs because of the π–π stacking between the π-electron systems of the aromatic molecules and the SWNT.[30] In fact, the functionalization of nanotubes with aromatic compounds by the π–π interactions has been frequently explored in order to construct nanotube composites and to solubilize the nanotubes in organic solvents.[31] Therefore, the formation of the densely adsorbed SWNT layer on the BT SAM, as shown in Figure 2a, was attributed to such a π–π stacking interaction. This result was consistent with the literature where nanotubes were immobilized on a SAM of phenyl-terminated silane.[23] In contrast, the 1PT molecule possessed no functional group that could have a strong interaction, such as a charge-transfer or a π–π stacking interaction, with the SWNT surface. Hence, it was expected that the nanotubes would be less strongly adsorbed on the 1PT SAM than on the 4AT or BT SAMs. We ascribed the formation of the mesh-like structure observed in Figure 2b to such a weak interaction of the SWNTs with the SAM. The weak interaction caused the high surface mobility of the nanotubes, which in turn facilitated their self-aggregation on the 1PT surface during the spin-coating procedure.

The nanotubes formed dense adlayers on the 4AT and BT SAMs and mesh-like adlayers on the 1PT SAM with high reproducibility. These adlayers uniformly covered the SAM surfaces over the entire investigated areas. Such reproducibility can be associated with the stability and uniformity of the thiolate SAMs.[32]

It was important to fine-tune the amount of uniformly dispersed nanotubes on the 4AT and BT SAMs from the viewpoint of practical application of the present method, such as the creation of nanotube electronic devices or sensors. To this end, we investigated the effects of the SWNT concentration of the spin-coating solution on the SWNT immobilization. SWNT concentrations of 0.1 and 0.01 mg mL^{-1} were tested for the immobilization on the 4AT and BT SAMs. When the moderately dilute SWNT solution, 0.1 mg mL^{-1}, was used for the spin coating, the nanotubes were sparsely immobilized on the 4AT SAM (Figure 3a). In contrast, the nanotubes still formed a densely immobilized layer on the BT SAM when the 0.1-mg mL^{-1} solution was used (Figure 3b). This difference in the SWNT concentration on the 4AT and BT SAMs demonstrated that the BT SAM adsorbed the nanotubes more strongly than the

4AT SAM. A comparison of the SWNT layers on the BT SAM prepared with the 1- and 0.1-mg mL^{-1} solutions (Figures 2a and 3b, respectively) revealed that the tubular structures of the nanotubes were frequently found in Figure 3b. This observation indicated that the SWNT density in the immobilized layer certainly decreased with a decrease in the solution concentration of the SWNT. In the case of the most dilute SWNT solution (0.01 mg mL^{-1}), only a few nanotubes were found on both the 4AT and the BT SAMs (see Supporting Information[33]).

In summary, the effect of the surface chemistry of SAMs on SWNT adsorption was investigated by AFM. A strong interaction of SWNT with 4AT or BT SAMs resulted in a uniformly dispersed attachment of the nanotubes on the SAMs. In contrast, a mesh-like structure of the SWNT was found on a 1PT SAM. We concluded that this structure was a result of the self-aggregation of the SWNTs on the surface caused by a weak interaction between the SWNT and the SAM. These results indicated that a rational design of the SAM functionality enabled one to control the surface assembly of the SWNTs.

References and Notes

1 R. H. Baughman, A. A. Zakhidov, W. A. de Heer, *Science* **2002**, *297*, 787.

2 P. Avouris, *Acc. Chem. Res.* **2002**, *35*, 1026.

3 J.-H. Ahn, H.-S. Kim, K. J. Lee, S. Jeon, S. J. Kang, Y. Sun, R. G. Nuzzo, J. A. Rogers, *Science* **2006**, *314*, 1754.

4 G. Gruner, *J. Mater. Chem.* **2006**, *16*, 3533.

5 J. Kong, N. R. Franklin, C. Zhou, M. G. Chapline, S. Peng, K. Cho, H. Dai, *Science* **2000**, *287*, 622.

6 E. S. Snow, F. K. Perkins, E. J. Houser, S. C. Badescu, T. L. Reinecke, *Science* **2005**, *307*, 1942.

7 M. W. Rowell, M. A. Topinka, M. D. McGehee, H.-J. Prall, G. Dennler, N. S. Sariciftci, L. Hu, G. Gruner, *Appl. Phys. Lett.* **2006**, *88*, 233506.

8 C. Li, Y. Chen, Y. Wang, Z. Iqbal, M. Chhowalla, S. Mitra, *J. Mater. Chem.* **2007**, *17*, 2406.

9 Y. Yan, M. B. Chan-Park, Q. Zhang, *Small* **2007**, *3*, 24.

10 L. Huang, Z. Jia, S. O'Brien, *J. Mater. Chem.* **2007**, *17*, 3863.

11 B. W. Smith, Z. Benes, D. E. Luzzi, J. E. Fischer, D. A. Walters, M. J. Casavant, J. Schmidt, R. E. Smalley, *Appl. Phys. Lett.* **2000**, *77*, 663.

12 J. Gao, A. Yu, M. E. Itkis, E. Bekyarova, B. Zhao, S. Niyogi, R. C. Haddon, *J. Am. Chem. Soc.* **2004**, *126*, 16698.

13 C. Kocabas, M. A. Meitl, A. Gaur, M. Shim, J. A. Rogers, *Nano Lett.* **2004**, *4*, 2421.

14 K. Keren, R. S. Berman, E. Buchstab, U. Sivan, E. Braun, *Science* **2003**, *302*, 1380.

15 H. Xin, A. T. Woolley, *J. Am. Chem. Soc.* **2003**, *125*, 8710.

16 M. D. Lay, J. P. Novak, E. S. Snow, *Nano Lett.* **2004**, *4*, 603.

17 H. Xin, A. T. Woolley, *Nano Lett.* **2004**, *4*, 1481.

18 Y. Guo, N. Minami, S. Kazaoui, J. Peng, M. Yoshida, T. Miyashita, *Physica B (Amsterdam, Neth.)* **2002**, *323*, 235.

19 Y. Kim, N. Minami, W. Zhu, S. Kazaoui, R. Azumi, M. Matsumoto, *Jpn. J. Appl. Phys.* **2003**, *42*, 7629.

20 M. C. LeMieux, S. Sok, M. E. Roberts, J. P. Opatkiewicz, D. Liu, S. N. Barman, N. Patil, S. Mitra, Z. Bao, *ACS Nano* **2009**, *3*, 4089.

21 J. P. Opatkiewicz, M. C. LeMieux, Z. Bao, *ACS Nano* **2010**, *4*, 1167.

22 Y. Wang, D. Maspoch, S. Zou, G. C. Schatz, R. E. Smalley, C. A. Mirkin, *Proc. Natl. Acad. Sci. U.S.A.* **2006**, *103*, 2026.

23 M. C. LeMieux, M. Roberts, S. Barman, Y. W. Jin, J. M. Kim, Z. Bao, *Science* **2008**, *321*, 101.

24 S. Giordani, S. D. Bergin, V. Nicolosi, S. Lebedkin, M. M. Kappes, W. J. Blau, J. N. Coleman, *J. Phys. Chem. B* **2006**, *110*, 15708.

25 P. Wagner, M. Hegner, H.-J. Güntherodt, G. Semenza, *Langmuir* **1995**, *11*, 3867.

26 T. Nishino, S. Kanata, Y. Umezawa, *Chem. Commun.* **2011**, *47*, 7467.

27 Y. Maeda, S.-i. Kimura, Y. Hirashima, M. Kanda, Y. Lian, T. Wakahara, T. Akasaka, T. Hasegawa, H. Tokumoto, T. Shimizu, H. Kataura, Y. Miyauchi, S. Maruyama, K. Kobayashi, S. Nagase, *J. Phys. Chem. B* **2004**, *108*, 18395.

28 J. Kong, H. Dai, *J. Phys. Chem. B* **2001**, *105*, 2890.

29 J. J. W. M. Rosink, M. A. Blauw, L. J. Geerligs, E. van der Drift, B. A. C. Rousseeuw, S. Radelaar, W. G. Sloof, E. J. M. Fakkeldij, *Langmuir* **2000**, *16*, 4547.

30 A. Nish, J.-Y. Hwang, J. Doig, R. J. Nicholas, *Nat. Nanotechnol.* **2007**, *2*, 640.

31 N. Nakashima, *Sci. Technol. Adv. Mater.* **2006**, *7*, 609.

32 A. Ulman, *Chem. Rev.* **1996**, *96*, 1533.

33 Supporting Information is available electronically on the CSJ-Journal Web site, http://www.csj.jp/journals/chem-lett/index.html.